FUDMA Journal of Engineering and Technology
ISSN: 3092-9385
https://fjet.fudutsinma.edu.ng/index.php/fjet/
Volume 2, Issue 2, 2026, 336-349

Design and Analysis of a Dual-Band Circular Microstrip Antenna Using Spatially Distributed CSRRs

Israel A. OLUWAFEMI[1*], Akaninyene B. OBOT[2], Emmanuel UBOM[3], Ayodele A. OLATUNJI[4], Mbuotidem G. ROBINSON[5]

[1*]Electrical and Electronic Engineering Department, Heritage Polytechnic, Eket, Akwa Ibom State
[2]Electrical and Electronic Engineering Department, University of Uyo, Uyo, Akwa Ibom State, Nigeria
[3]Telecommunication Engineering Department, Akwa Ibom State University, Ikot Akpaden, Akwa Ibom State, Nigeria
[4]Electrical and Electronic Engineering Department, Michael Okpara University of Agriculture, Umudike, Nigeria
[5]Electrical and Electronic Engineering Department, Federal University of Technology, Ikot Abasi, Akwa Ibom State, Nigeria

[1*]iaoluwafemi@heritagepoly.edu.ng, [2]akaninyeneobot@uniuyo.edu.ng, [3]emmanuelubom@aksu.edu.ng, [4]olatunji_ayodele@mouau.edu.ng, [5]ferireo@gmail.com

Abstract
Previous studies on metamaterial-integrated Circular Microstrip Antennas (CMSAs) for 5G applications have reported improvements in radiation characteristics, while bandwidth enhancement has remained a design challenge. This study investigates the effect of Complementary Split-Ring Resonator (CSRR) number and spatial arrangement on the impedance characteristics of a circular microstrip antenna operating over 3.4–4.2 GHz. The antenna was designed and simulated using CST Studio Suite on an FR-4 substrate with a relative permittivity of 4.4 and thickness of 1.6 mm. A conventional CMSA was first established as the baseline, after which several CSRR configurations involving the circular patch and ground plane were investigated. The selected configuration consists of one CSRR incorporated into the circular patch and three CSRRs arranged in a ">" configuration on the ground plane. The resulting antenna exhibits two −10 dB impedance bands from 3.7056–3.8848 GHz and 3.984–4.200 GHz, corresponding to bandwidths of 179.2 MHz and 216.0 MHz, respectively. Within the simulated frequency range, the aggregate accepted bandwidth is 395.2 MHz, compared with 352.8 MHz for the baseline CMSA. The selected configuration also produces a maximum simulated directivity of 5.265 dBi at 3.9 GHz. The comparative results show that the impedance response is strongly affected by the number and spatial distribution of the CSRRs. The simulation results show that an appropriate spatial arrangement of CSRRs can provide dual-band operation while maintaining satisfactory simulated radiation characteristics.

Keywords: *Dual band, Circular microstrip antenna, CSRR, Bandwidth, Directivity, 5G.*

1.0 Introduction

The deployment of Fifth-Generation (5G) wireless communication systems has increased the demand for compact antenna structures with suitable impedance bandwidth and radiation characteristics for operation within designated frequency bands. Microstrip antennas remain attractive for wireless communication applications because of their low-profile geometry, ease of integration, and relatively simple fabrication. However, conventional microstrip antennas generally exhibit limited impedance bandwidth, which can restrict their use in applications requiring wider or multiple operating bands [1].

Among the various microstrip antenna configurations, the Circular Microstrip Antenna (CMSA) is attractive because of its compact geometry, ease of fabrication, and suitability for integrated wireless systems. Its electromagnetic performance, however, depends on parameters including substrate properties, patch dimensions, feeding arrangement, and operating frequency. Consequently, several techniques have been investigated to modify the impedance and radiation characteristics of microstrip antennas.

Metamaterials provide a means of modifying electromagnetic behaviour through artificially engineered structures and have been widely investigated for antenna performance enhancement, miniaturisation, and bandwidth improvement [2], [3]. Among the resonant structures used in metamaterial-based microwave designs, Complementary Split-Ring Resonators (CSRRs) are particularly useful because their geometry can introduce additional resonant behaviour when incorporated into planar electromagnetic structures. The resonant response of a CSRR-loaded antenna is influenced by the dimensions, position, and electromagnetic coupling of the resonator with the host antenna [4], [5].

Recent studies have demonstrated the ability of CSRR loading to generate or modify multiple resonant responses in antennas designed for sub-6 GHz applications. Shobana [4] developed a CSRR-loaded microstrip antenna for sub-6 GHz 5G applications in which co-directional CSRRs produced dual resonances covering the n78 and n79 5G NR frequency regions. The study also used parametric analysis to relate the geometrical

Received: 22/08/2026; Revised: 28/08/2026; Accepted: 28/08/2026; Published: 31/08/2026

dimensions of the antenna and CSRR to the resulting return-loss response. Barad *et al.* [5] subsequently demonstrated a CSRR-loaded microstrip patch element operating at 3.45 and 3.87 GHz as part of a dual-band sub-6 GHz phased-array antenna. Their study included a sensitivity analysis of CSRR position and excitation position and showed that the CSRR-loaded patch could produce dual-band behaviour through electromagnetic coupling between the resonator and the patch. More recently, Andrews *et al.* [6] investigated a CSRR incorporated into the ground plane of a compact FR-4 antenna and reported a shift of the resonant frequency to approximately 3.5 GHz with a simulated impedance bandwidth of 200 MHz.

Recent investigations have further demonstrated the usefulness of CSRR loading for controlling dual-band and multiband behaviour in sub-6 GHz antenna systems. Barad et al. [7] reported a dual-band, dual-polarized sub-6 GHz phased-array antenna with CSRR-loaded patch elements operating at 3.45 and 3.87 GHz. Their study also examined the effect of CSRR and excitation positions through sensitivity analysis, reinforcing the importance of the spatial relationship between the resonator and the host patch in determining the resulting electromagnetic response. The reported agreement between simulated and measured results further demonstrates the practical relevance of CSRR-based dual-band antenna designs [7].

More recent studies have continued to apply CSRR structures to obtain controlled frequency responses in the sub-6 GHz region. Chandrasekhar and Naik [8] developed a CSRR-loaded patch array with two operating bands at 3.06–3.16 GHz and 4.36–4.47 GHz, showing that resonator loading can be used to establish separated operating regions. Varshney et al. [9] similarly used a CSRR in a compact metasurface antenna to introduce a controlled notch and obtain isolated sub-6 GHz operating bands, while Anusha and Mohana Geetha [10] investigated SRR and CSRR loading together with parametric and optimization-based design approaches for multiband sub-6 GHz operation. In another recent study, Basavaraju and Ramanujam [11] incorporated a circular CSRR into a fabricated multiband antenna and reported additional resonance generation within the sub-6 GHz range. These recent investigations show that CSRR geometry, loading location, and interaction with other antenna features continue to be important considerations in the control of resonant behaviour and impedance characteristics.

These studies establish that CSRR loading can modify the resonant frequency, impedance bandwidth, and multiband behaviour of microstrip antennas. They also show that CSRR geometry and location are important electromagnetic design variables. However, comparatively limited attention has been given to the effect of distributing multiple CSRR elements between the radiating patch and the ground plane of a Circular Microstrip Antenna. This provides the specific motivation for the present study.

In an earlier study, Oluwafemi *et al.* [12] investigated the integration of CSRR-based metamaterials into Circular Microstrip Antennas for 5G applications. The study established that the circular microstrip configuration exhibited superior performance compared with the rectangular microstrip configuration and further demonstrated that metamaterial integration improved the gain and radiation characteristics of the antenna. However, the results also revealed an important limitation. Although improvement in radiation performance was obtained, the bandwidth remained limited for wider sub-6 GHz applications [12]. This result provided the immediate motivation for the present investigation.

The present study therefore extends the previous work by examining the effect of CSRR number and spatial distribution on the electromagnetic response of a CMSA. Multiple CSRR structures are introduced at different locations on the circular patch and ground plane, and representative configurations are comparatively investigated using full-wave electromagnetic simulation. Particular attention is given to the effects of CSRR placement on resonant frequency, impedance matching, bandwidth, and radiation characteristics.

Unlike the previous study, which primarily examined the effect of metamaterial integration on the CMSA, the present work investigates how the geometric arrangement of multiple CSRR structures influences antenna behaviour. The study does not employ a formal numerical optimisation algorithm. Instead, different CSRR configurations are simulated and compared to identify an arrangement capable of providing dual-band operation with satisfactory impedance and radiation characteristics.

The principal contribution of this work is the comparative simulation-based analysis of a specific spatial CSRR configuration consisting of one CSRR incorporated into the circular patch and three CSRRs arranged in a ">" configuration on the ground plane. The selected configuration exhibited two simulated −10 dB impedance bands from 3.7056–3.8848 GHz and 3.984–4.200 GHz, corresponding to bandwidths of 179.2 MHz and 216 MHz, respectively. The combined accepted bandwidth of the two separated operating bands is 395.2 MHz, compared with 352.8 MHz for the baseline CMSA.

The practical relevance of the proposed configuration lies in its ability to provide two separated simulated impedance bands within the investigated sub-6 GHz frequency range using a single circular microstrip antenna. This characteristic is relevant to 5G antenna applications where operation across more than one frequency region can be useful without requiring separate antenna elements for each band. The study therefore contributes a spatial CSRR-loading approach for controlling the resonant response of the CMSA, while showing that the location and distribution of the resonators can be used as design variables for obtaining the desired dual-band response.

Received: 22/08/2026; Revised: 28/08/2026; Accepted: 28/08/2026; Published: 31/08/2026

The comparative investigation further shows that the antenna response is affected not only by the presence of CSRR structures but also by their number, location, and geometric distribution within the antenna. The observed differences among the investigated configurations provide the basis for selecting the final arrangement and for interpreting the resulting dual-band response.

The remainder of this paper presents the essential theoretical relationships used in the CMSA and CSRR design, followed by the simulation methodology, comparative analysis of the investigated configurations, detailed discussion of the selected configuration, and conclusions.

2.0 Theoretical Analysis

2.1 Circular Microstrip Antenna

A circular microstrip antenna consists of a conducting circular patch separated from a conducting ground plane by a dielectric substrate. Its resonant behaviour is governed primarily by the patch dimensions, substrate permittivity and thickness, and feeding arrangement. For the present design, an FR-4 substrate with a relative permittivity of 4.4 and thickness of 1.6 mm was used. The circular patch has a radius of 10.58 mm, while the antenna was designed around a centre frequency of 3.8 GHz within the investigated 3.4–4.2 GHz frequency range.

The conventional CMSA serves as the reference structure in this study. Its dimensions and feed-line parameters were first established before introducing the metamaterial structures. The final feed-line width used in the simulations was 3.083 mm, with a 50 Ω transmission-line interface.

The baseline antenna provides the reference electromagnetic response against which the CSRR-loaded configurations are evaluated. This is important because the objective of the present study is not simply to demonstrate that CSRR loading produces a resonance, but to determine how the number and spatial distribution of CSRRs modify the response of an established CMSA.

2.2 Electromagnetic Principle of the CSRR

A Complementary Split-Ring Resonator is formed by etching complementary split-ring slots into a conducting surface. The structure behaves as a resonant electromagnetic element whose response is determined primarily by its effective inductance and capacitance. CSRRs have been widely investigated in microwave and antenna structures because their resonant behaviour can be used to modify impedance characteristics, introduce additional resonant responses, and control the frequency response of planar structures [2], [13], [14].

The fundamental resonant behaviour of an idealised resonant structure can be represented by the LC relationship

$$f_r = \frac{1}{2\pi\sqrt{LC}} \quad (1)$$

where L represents the effective inductance and C represents the effective capacitance of the resonant structure.

For a CSRR, the effective capacitance is influenced by parameters such as the ring dimensions, slot width, separation between the rings, and split-gap dimensions. The inductive behaviour is similarly dependent on the current path and physical dimensions of the resonator. Consequently, changing the CSRR geometry changes its natural resonant frequency.

For the present antenna, the CSRR dimensions were initially selected with reference to the target frequency range and subsequently adjusted through CST simulation. The final CSRR dimensions are an outer ring radius of 4.0 mm, inner ring radius of 3.0 mm, ring width of 0.5 mm, inter-ring spacing of 0.5 mm, and split gap of 0.5 mm.

2.3 CSRR Coupling with the CMSA

The presence of a CSRR does not create an independent resonance that is completely isolated from the circular patch. When the resonator is incorporated into the antenna structure, electromagnetic coupling occurs between the CSRR and the fields and currents associated with the CMSA.

The resulting antenna can therefore be considered as a coupled resonant system consisting of the original CMSA mode and one or more CSRR-associated modes. In simplified form, the interaction may be represented by

$$\omega_0 \leftrightarrow \omega_r$$

where ω0 is the natural angular frequency of the CMSA and ωr is the natural angular frequency of the CSRR.

The strength of this interaction depends on the location and orientation of the CSRR relative to the electromagnetic field distribution of the host antenna. A CSRR positioned in a region of significant electric or surface-current interaction can couple more strongly with the antenna mode than an identical resonator positioned in a weak-field region. Recent CSRR antenna studies have similarly shown that resonator position and coupling can significantly affect the resulting resonant response [4], [5].

This provides the theoretical basis for the configuration study undertaken in this work. The CSRRs are not treated merely as additional geometric features. Their number, location and spatial arrangement are regarded as variables that modify the electromagnetic coupling within the CMSA.

Received: 22/08/2026; Revised: 28/08/2026; Accepted: 28/08/2026; Published: 31/08/2026

2.4 Effect of Multiple CSRRs

When several CSRRs are incorporated into an antenna, their combined effect depends on both their individual resonant characteristics and their mutual electromagnetic interaction. Increasing the number of CSRRs does not necessarily produce the same number of observable resonant frequencies because the resulting response depends on the coupling strength and relative position of the resonators. Consequently, configurations containing similar numbers of CSRRs may exhibit substantially different S11, VSWR, and bandwidth characteristics.

This consideration is particularly important in the present study because CSRRs are distributed between the circular patch and the ground plane. A CSRR incorporated into the patch interacts primarily with the electromagnetic behaviour of the radiating structure, whereas a CSRR incorporated into the ground plane modifies the electromagnetic environment associated with the return-current path and the patch-ground interaction. The resulting response therefore depends on the distribution of resonators between these two regions.

2.5Spatial Arrangement and Dual-Band Response

The dual-band behaviour investigated in this work is interpreted as the result of interaction between the fundamental CMSA resonance and additional resonant behaviour introduced by the CSRR loading. When the resonant frequencies and coupling conditions are suitably related, the combined structure can exhibit more than one frequency region satisfying the specified impedance-matching criterion.

The spatial arrangement of the CSRRs therefore becomes an important design variable. Changing the number of resonators, their position on the patch, their position on the ground plane, or their relative spacing changes the electromagnetic coupling and consequently modifies the S11 response.

This provides the theoretical basis for comparing the different configurations investigated in this study. The subsequent simulation analysis therefore considers the CSRR arrangement as a principal design variable rather than treating the final geometry as an isolated design.

2.6 Antenna and CSRR Design Parameters

The final dimensions used for the CMSA and CSRR-loaded structure are retained for reproducibility. The principal parameters are summarised in Table 1.

Table 1. Principal dimensions of the CMSA and CSRR

Parameter	Value
Substrate	FR-4
Relative permittivity, εr	4.4
Substrate thickness, h	1.6 mm
Patch diameter	21.16 mm
Patch radius	10.58 mm
Ground-plane diameter	42.32 mm
Patch thickness	0.036 mm
Ground-plane thickness	0.036 mm
Feed-line width	3.083 mm
Feed-line length	18.26 mm
CSRR outer radius	4.0 mm
CSRR inner radius	3.0 mm
CSRR ring width	0.5 mm
CSRR inter-ring spacing	0.5 mm
CSRR split gap	0.5 mm

These values correspond to the final antenna dimensions used in the simulations.

3.0 Simulation Methodology

3.1 The Simulation Procedure

The antenna configurations were designed and analysed using CST Studio Suite. The investigation was conducted in stages, beginning with the design and simulation of a conventional Circular Microstrip Antenna (CMSA) without metamaterial loading. This antenna served as the baseline structure against which the CSRR-loaded configurations were evaluated.

After establishing the baseline response, CSRRs were introduced into the antenna structure at selected positions on the circular radiating patch and ground plane. The purpose of the configuration study was to examine how the number and spatial distribution of the CSRRs affect the impedance response and radiation characteristics of the CMSA.

Received: 22/08/2026; Revised: 28/08/2026; Accepted: 28/08/2026; Published: 31/08/2026

Rather than applying a formal numerical optimisation algorithm, the study used a comparative full-wave simulation approach. Several geometrically distinct CSRR arrangements were modelled while maintaining the principal antenna and CSRR dimensions described in Section 2. For each configuration, the simulated S11, VSWR, impedance bandwidth, and radiation characteristics were examined. The −10 dB reflection-coefficient criterion was used to determine the impedance bandwidth of each configuration.

The configuration study was designed to distinguish the effect of CSRR loading from the effect of CSRR **arrangement**. Consequently, configurations containing different numbers of resonators and different distributions between the patch and ground plane were considered. The representative configurations investigated in the study are summarised in Table 2.

Table 2. Representative CSRR configurations investigated

Configuration	Patch CSRRs	Ground CSRRs	Arrangement	Total
C1	1	3	“>”	4
C2	4	3	“<”	7
C3	1	3	“\”	4
C4	2	3	“<”	5

Note: The configurations are distinguished by the number and spatial distribution of CSRRs. The exact geometric arrangement of each configuration is shown in the corresponding CST models.

3.2 Configuration Evaluation

Each configuration was simulated over the frequency range of 3.4–4.2 GHz. The baseline CMSA was first evaluated to establish its reference impedance response and bandwidth. The CSRR-loaded configurations were then evaluated under the same simulation conditions to ensure that the comparison was based on the same frequency range, substrate, antenna dimensions, and excitation conditions.

The primary selection criterion was the impedance response obtained from the S_{11} parameter. A frequency region was considered part of the operating bandwidth when

$$S_{11} \leq -10 \text{ dB}.$$

The corresponding bandwidth was calculated as

$$BW = f_H - f_L \tag{2}$$

where f_H and f_L are the upper and lower frequencies, respectively, at which the $S_{11} = -10$ dB criterion is satisfied.

In addition to impedance bandwidth, the configurations were examined for the occurrence of multiple resonant regions, VSWR behaviour, and radiation characteristics. A configuration was considered favourable when it produced a useful dual-band response while maintaining satisfactory radiation characteristics within the investigated frequency range.

This procedure provided a common basis for comparing the different CSRR arrangements rather than selecting the final geometry solely from a visual inspection of the antenna response.

3.3 Baseline CMSA

The conventional CMSA was simulated first without CSRR loading. This structure provided the reference against which the effects of subsequent CSRR integration were assessed.

The baseline antenna was designed with an FR-4 substrate having a relative permittivity of 4.4 and thickness of 1.6 mm. The circular patch has a radius of 10.58 mm, and the antenna operates within the investigated 3.4–4.2 GHz frequency range. The feed line has a width of 3.083 mm and provides a 50 Ω interface. These dimensions are retained for the CSRR-loaded configurations so that changes in the simulated response can be attributed primarily to the CSRR arrangement.

The baseline CMSA produced an effective impedance bandwidth of 352.8 MHz, extending from 3.4264 to 3.7792 GHz under the −10 dB reflection-coefficient criterion.

This baseline result establishes the reference against which the dual-band behaviour of the selected CSRR configuration is subsequently assessed.

3.4 CSRR Configuration Study

The CSRR-loaded designs were developed by introducing resonators into the circular patch and ground plane in different spatial arrangements. The configuration study was motivated by the electromagnetic mechanism discussed in Section 2, whereby the position of a resonator relative to the antenna fields and surface currents can influence the strength of electromagnetic coupling and, consequently, the resulting impedance response.

The first group of configurations investigated increased CSRR loading on the ground plane while maintaining multiple resonators on the patch. Other configurations altered the relative distribution of the resonators between the two regions. These changes resulted in visibly different S11 and VSWR responses, indicating that the electromagnetic response was sensitive to the geometric arrangement rather than simply to the presence of metamaterial loading.

Figure 1 presents the geometrical configurations of the four representative CSRR-loaded circular microstrip antennas considered in this study. The configurations employ different numbers and spatial arrangements of CSRRs on the radiating patch and ground plane while retaining the same basic antenna structure. C1 represents the principal candidate arrangement, whereas C2–C4 provide alternative spatial distributions for comparative evaluation. These configurations were selected from the broader set of investigated designs based on their simulated impedance characteristics and suitability for further performance analysis. Both the three-dimensional antenna structures and the corresponding top-view CSRR arrangements are shown.

The four configurations provide a basis for examining the influence of CSRR number, location, and spatial distribution on the electromagnetic response of the CMSA. Their comparison enables the effects of patch-side and ground-plane loading, individually and in combination, to be evaluated through the simulated S11, VSWR, bandwidth, and radiation characteristics. The results of this comparative assessment provide the basis for identifying the configuration selected for subsequent detailed analysis.

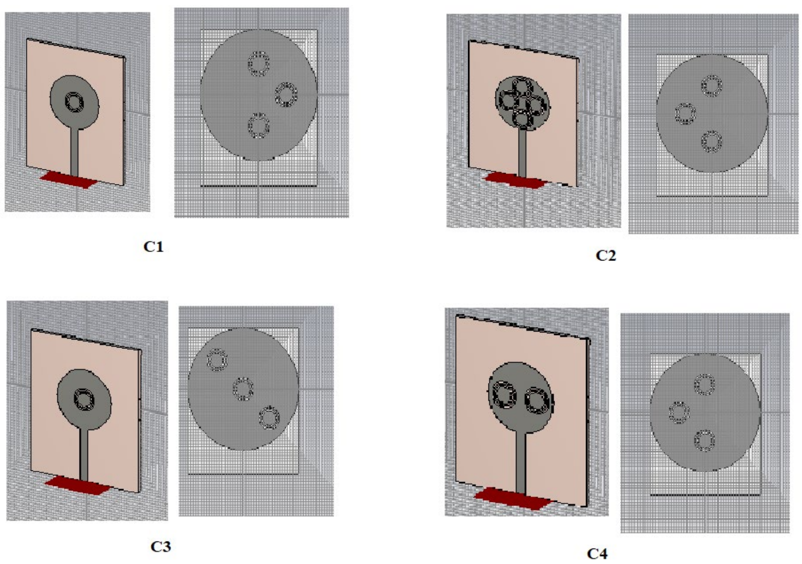

Figure 1. Geometrical configurations and spatial arrangements of CSRRs for the four selected circular microstrip antenna designs (C1–C4).

3.5 Selection of the Proposed Configuration

Following the comparative simulation of the representative configurations, the configuration containing one CSRR on the circular patch and three CSRRs on the ground plane was selected for detailed analysis.

The three ground-plane CSRRs were arranged in a ">" configuration, with two resonators positioned vertically and the third positioned to the right. This arrangement was retained for the final design because it produced two distinct impedance-matched regions within the investigated frequency range.

The selected configuration produced the following −10 dB impedance bands:

3.7056–3.8848 GHz

and

3.984–4.200 GHz.

The corresponding bandwidths are 179.2 MHz and 216 MHz, respectively. The detailed performance of this configuration is presented in Section 4.

4.0 Results and Discussion

4.1 Impedance Characteristics and −10 dB Bandwidth

The simulated impedance characteristics of the selected CSRR-loaded CMSA configurations were evaluated from their input reflection coefficient, S11, over the frequency range of 3.4–4.2 GHz. The −10 dB criterion was adopted to identify the impedance-matched operating regions. For each configuration, the minimum S11, the corresponding resonant frequency, the individual impedance bandwidths, and the number of distinct matched bands were determined from the CST simulation data.

The four configurations exhibit markedly different impedance responses despite being based on the same CMSA and CSRR dimensions. This difference is important because the configurations do not differ only in the total number of CSRRs. Their distribution between the circular patch and ground plane, together with the spatial

Received: 22/08/2026; Revised: 28/08/2026; Accepted: 28/08/2026; Published: 31/08/2026

arrangement of the ground-plane resonators, is also different. The results therefore provide a direct basis for examining the influence of CSRR arrangement on the impedance behaviour of the antenna.

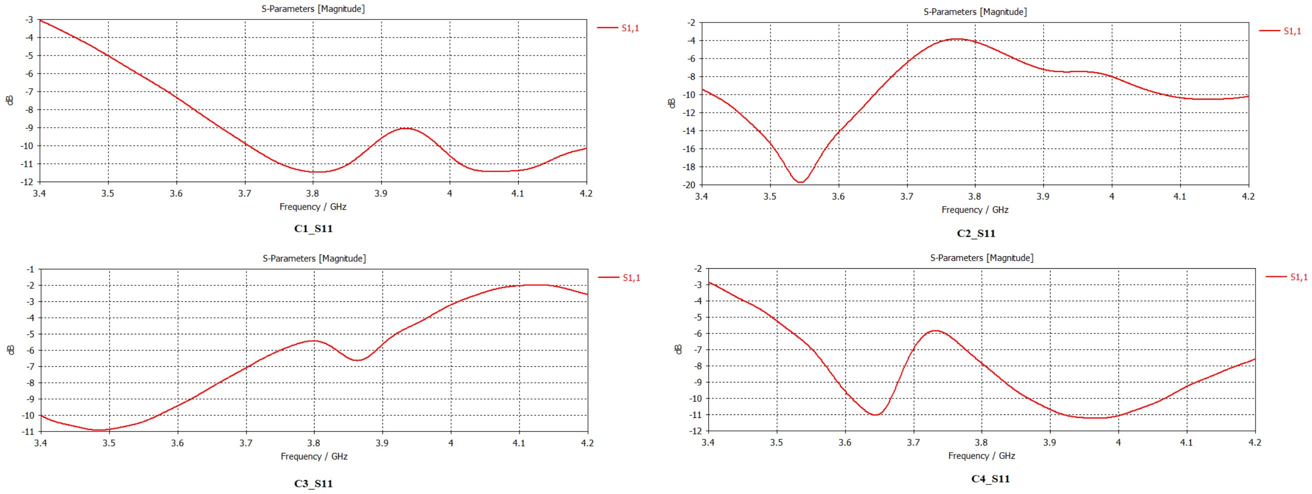

Figure 2. Simulated S11 responses of configurations C1-C4 over 3.4–4.2 GHz

The numerical results extracted from the CST data are summarised in Table 3.

Table 3. Impedance characteristics of the selected CSRR configurations.

Configuration	Patch CSRRs	Ground CSRRs	Arrangement	Total CSRRs	Minimum S11 (dB)	−10 dB bandwidth	Number of bands
C1	1	3	“>”	4	−11.469	395.2 MHz	2
C2	4	3	“<”	7	−10.922	171.2 MHz	1
C3	1	3	“\”	4	−11.476	394.4 MHz	2
C4	2	3	“<”	5	−19.749	361.6 MHz	2

The C1 configuration produces two impedance-matched regions, extending from approximately 3.7056 to 3.8848 GHz and from 3.9840 to 4.2000 GHz. The minimum S11 is approximately −11.47 dB at 3.8072 GHz. The two matched regions provide a combined bandwidth of approximately 395.2 MHz within the simulated frequency range.

C2 exhibits a different response. Although it contains seven CSRRs, its S11 response produces only one identifiable −10 dB region, extending from the lower simulation boundary at 3.4 GHz to approximately 3.5712 GHz. Its minimum S11 is approximately −10.92 dB at 3.4848 GHz.

C3, despite having the same total number of CSRRs as C1, produces a response very similar to C1. It provides two matched regions, approximately 3.7064–3.8856 GHz and 3.9848–4.2000 GHz. The minimum S11 is approximately −11.48 dB at 3.8072 GHz. The resulting combined bandwidth within the simulated range is approximately 394.4 MHz.

C4 produces the deepest impedance minimum among the four configurations, reaching approximately −19.75 dB at 3.5440 GHz. It also produces two matched regions. The first extends approximately from 3.4152 to 3.6512 GHz, while the second begins at approximately 4.0744 GHz and continues to the upper simulation boundary of 4.2 GHz. The combined bandwidth within the investigated range is approximately 361.6 MHz.

Interpretation

The results reveal an important feature of the configuration study. The number of CSRRs alone does not determine the impedance response. C1 and C3 both contain four CSRRs, with one resonator on the patch and three on the ground plane, yet their ground-plane arrangements are different. Nevertheless, both produce almost the same total matched bandwidth and nearly identical minimum S11. This makes their comparison particularly valuable for investigating the effect of spatial arrangement.

C2 provides an even stronger indication that increasing the number of CSRRs does not necessarily improve antenna performance. It contains seven CSRRs, the largest loading among C1-C4, but produces only one −10 dB band within the investigated range. Its minimum S11 is also only slightly below the −10 dB criterion.

C4, on the other hand, produces the deepest impedance minimum despite containing fewer CSRRs than C2. This suggests that the electromagnetic coupling produced by the location and arrangement of the resonators can be more important than their numerical quantity alone.

Received: 22/08/2026; Revised: 28/08/2026; Accepted: 28/08/2026; Published: 31/08/2026

This observation is consistent with the theoretical treatment in Section 2, where the CSRR response was related to its coupling with the electromagnetic fields and surface-current distribution of the host antenna. The configuration study therefore provides numerical evidence for treating CSRR geometry and spatial distribution as important design variables.

4.2 VSWR Comparison of C1-C4

VSWR provides a complementary assessment of the impedance-matching behaviour observed from the S11 responses. A lower VSWR indicates better power transfer from the feed to the antenna, with a value of 1 representing an ideal match. In practical antenna operation, VSWR values below 2 are generally regarded as indicative of acceptable impedance matching.

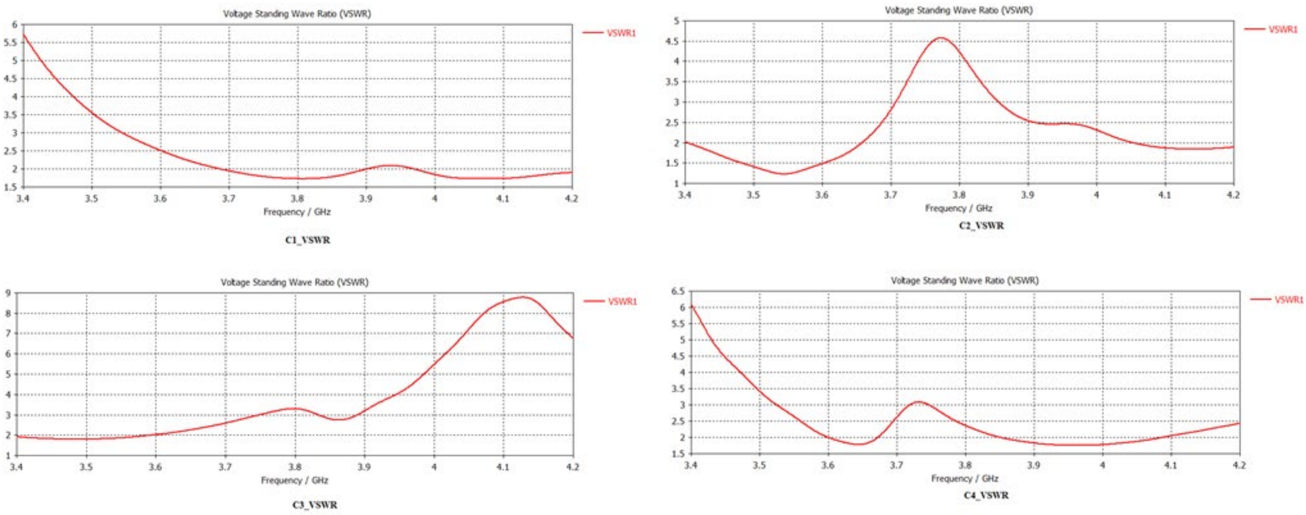

Figure 3 presents the simulated VSWR responses of configurations C1-C4 over the 3.4-4.2 GHz frequency range

The four configurations exhibit distinctly different impedance-matching characteristics despite having the same operating frequency range. C1 maintains a relatively low VSWR across a substantial portion of the band. Its response reaches approximately 1.7 at around 3.8 GHz and remains close to this value toward 4.1 GHz. This indicates relatively stable impedance matching around the principal operating region.

C2 exhibits the lowest VSWR among the four configurations. Its minimum value is approximately 1.2 at about 3.55 GHz. However, the VSWR rises sharply around 3.7-3.8 GHz, reaching approximately 4.5. The response subsequently falls again toward the upper part of the band. Thus, although C2 achieves excellent matching near its lower-frequency resonance, its matching behaviour is less stable across the complete frequency range.

C3 shows a VSWR close to 1.8 around 3.5 GHz, after which the value gradually increases. A second local minimum occurs around 3.85 GHz, where the VSWR is approximately 2.7. The rapid increase beyond approximately 3.9 GHz indicates deteriorating impedance matching toward the upper end of the investigated band.

C4 provides a comparatively stable response around the principal operating region. Its VSWR falls from approximately 6.0 at 3.4 GHz to about 1.8 around 3.9-4.0 GHz, before increasing gradually toward 4.2 GHz. This behaviour corresponds reasonably well with the S11 response observed for C4.

Table 4. VSWR characteristics of configurations C1-C4

Configuration	Minimum VSWR	Approx. frequency of minimum VSWR	VSWR behaviour around 3.8 GHz	VSWR behaviour around 4.0 GHz
C1	≈1.7	≈3.8 GHz	Low	Low
C2	≈1.2	≈3.55 GHz	High	≈2.4
C3	≈1.8	≈3.5 GHz	≈2.7	Increasing
C4	≈1.8	≈3.9-4.0 GHz	≈2.4	≈1.8

Interpretation

The VSWR results reinforce the observation from the S11 comparison that the spatial arrangement of the CSRRs has a substantial effect on the impedance characteristics of the antenna. The configurations do not simply produce a uniform improvement in matching. Instead, changing the CSRR arrangement shifts the locations of favourable and unfavourable matching regions.

Received: 22/08/2026; Revised: 28/08/2026; Accepted: 28/08/2026; Published: 31/08/2026

Of particular interest is C1, which combines a relatively low VSWR with a broad region of comparatively stable matching around the target frequency. This provides further justification for selecting C1 for the subsequent investigation of directivity, gain, efficiency and far-field radiation characteristics.

The behaviour of C2 is also significant. Although it produces the lowest individual VSWR minimum, that minimum occurs near 3.55 GHz and is followed by a pronounced deterioration in matching around 3.7-3.8 GHz. Therefore, the lowest VSWR value alone should not be used as the basis for selecting the optimum configuration.

This is an important point for the paper because it supports the use of multi-parameter evaluation rather than selecting a configuration solely from its deepest S11 minimum.

4.3 Directivity, Gain and Efficiency of C1

Table 5. Simulated radiation and impedance characteristics of C1

Frequency (GHz)	Directivity (dBi)	Radiation Efficiency (dB)	Total Efficiency (dB)	Calculated Gain (dBi)	S11 (dB)	VSWR
3.7	4.925	−1.152	−1.625	**3.773**	−9.865	1.946
3.8	5.009	−1.140	−1.462	**3.869**	−11.461	1.730
3.9	5.265	−1.497	−2.005	**3.768**	−9.571	1.995
4.0	5.087	−1.393	−1.793	**3.694**	−10.559	1.843
4.1	4.987	−1.098	−1.426	**3.889**	−11.380	1.739
4.2	5.024	−1.059	−1.500	**3.965**	−10.149	1.902

Table 5 presents the radiation and impedance characteristics at selected frequencies covering the two operating bands and the intervening transition region.

The radiation characteristics of the selected C1 configuration were evaluated over the frequency range containing its two impedance-matched operating regions. Table 5 presents the corresponding directivity, radiation efficiency, total efficiency, calculated gain, S11, and VSWR values. The inclusion of both impedance and radiation parameters allows the effect of frequency on the overall antenna performance to be assessed rather than relying on any single parameter.

The relationship between antenna gain, directivity, and radiation efficiency was also considered in evaluating the radiation performance of the proposed configurations. Antenna gain is related to directivity and radiation efficiency by

$$G = D\eta rad \tag{3}$$

where G is the antenna gain, D is the directivity, and ηrad is the radiation efficiency expressed as a linear ratio. When expressed in decibels, the relationship becomes

$$GdBi = DdBi + \eta rad,dB. \tag{4}$$

Equations (4) and (5) were used to calculate the gain values reported for C1 from the simulated directivity and radiation efficiency, and to interpret the relationship between these radiation parameters.

At 3.8 GHz, which lies within the lower operating band, C1 exhibits a directivity of 5.009 dBi, radiation efficiency of −1.140 dB, total efficiency of −1.462 dB, and calculated gain of 3.869 dBi. The corresponding S11 is −11.461 dB, with a VSWR of 1.730, confirming acceptable impedance matching at this frequency. The combination of relatively high directivity, good radiation efficiency, and low VSWR indicates that the antenna maintains satisfactory radiation performance within the lower operating band.

The directivity reaches its highest value of 5.265 dBi at 3.9 GHz. However, this frequency falls in the narrow transition region between the two −10 dB operating bands, where the S11 value rises to approximately −9.571 dB. Consequently, the high directivity observed at 3.9 GHz should not be interpreted as the optimum operating condition based on impedance matching. This observation demonstrates that maximum directivity and optimum impedance matching do not necessarily occur at the same frequency.

The results at 3.7 and 3.9 GHz are also significant in defining the separation between the two impedance-matched operating regions. At 3.7 GHz, the S11 value is −9.865 dB, which is slightly above the −10 dB criterion and therefore falls just outside the lower accepted band. As the frequency increases, the response enters the lower matched region and reaches −11.461 dB at 3.8 GHz. At 3.9 GHz, although the antenna exhibits its maximum directivity of 5.265 dBi, S11 rises again to −9.571 dB, placing this frequency in the transition region between the two accepted bands. The shallow rise of S11 above −10 dB around this region separates the two matched intervals. Without this intervening loss of impedance matching, the response would have constituted a wider continuous matched band rather than two distinct operating bands. Thus, the distinction between maximum radiation performance and impedance-defined operating bandwidth is important in interpreting the C1 response.

Within the upper operating band, the antenna maintains acceptable impedance matching throughout the investigated region. At 4.0 GHz, C1 records a directivity of 5.087 dBi, radiation efficiency of −1.393 dB, total efficiency of −1.793 dB, and calculated gain of 3.694 dBi, with S11=−10.559 dB and VSWR = 1.843. At 4.1 GHz, the directivity is 4.987 dBi, while the radiation and total efficiencies improve to −1.098 dB and −1.426 dB, respectively. The calculated gain increases to 3.889 dBi, accompanied by S11= −11.380 dB and VSWR = 1.739.

At 4.2 GHz, which represents the upper limit of the simulated frequency range, C1 exhibits a directivity of 5.024 dBi and the highest radiation efficiency among the sampled frequencies, approximately −1.059 dB. Consequently, the calculated gain increases to 3.965 dBi, the highest value in Table 5. The corresponding S11 of −10.149 dB and VSWR of 1.902 indicate that the antenna remains within the acceptable impedance-matching criterion at the upper simulation limit.

The results therefore show that the electromagnetic performance of C1 is frequency dependent. The frequency of maximum directivity does not coincide with the frequency of maximum calculated gain. The highest directivity occurs at 3.9 GHz, whereas the highest calculated gain within the sampled frequencies occurs at 4.2 GHz. This difference arises because gain depends on both the directional concentration of the radiation and the radiation efficiency. The results consequently indicate that directivity, efficiency, impedance matching, and gain should be considered together when assessing the performance of the CSRR-loaded CMSA.

The far-field radiation characteristics within the two operating bands provide a complementary view of the results in Table 5.

The three-dimensional far-field results provide a complementary view of the numerical results presented in Table 5. For the lower operating band, the 3.8 GHz result is selected because it lies within the −10 dB impedance bandwidth and provides a favourable combination of directivity, radiation efficiency, gain, and VSWR.

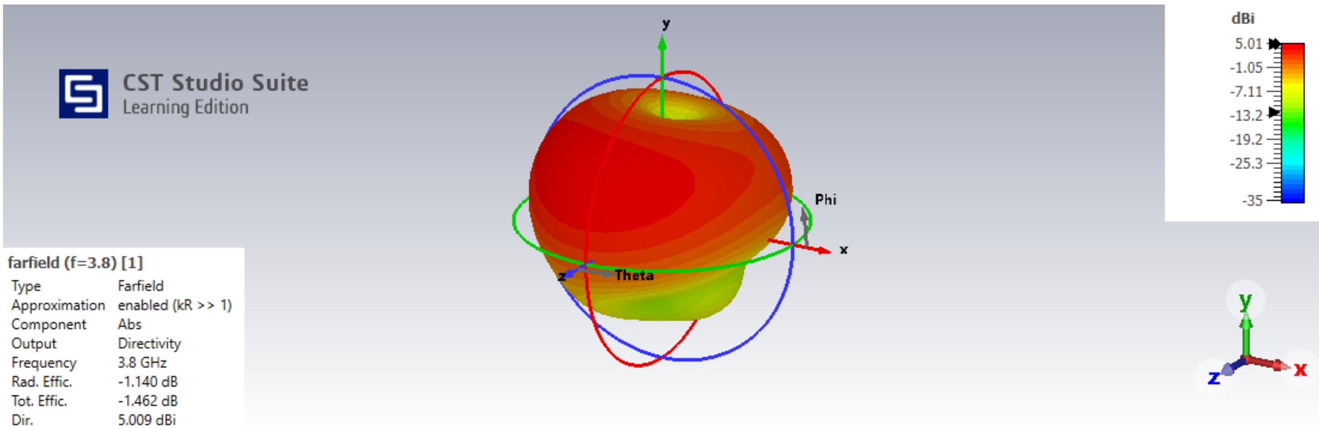

Figure 4: C1 three-dimensional far-field radiation pattern at 3.8 GHz

The 3.8 GHz far-field pattern should therefore be discussed as the representative radiation characteristic of C1 within the lower operating band. Its directivity of approximately 5.009 dBi, together with a radiation efficiency of approximately 76.9% after conversion from the CST dB value, indicates that the simulated antenna maintains useful radiation performance at this operating point.

For the upper operating band, 4.1 GHz provides a particularly useful representative point. At this frequency, C1 has S11=−11.380 dB and VSWR = 1.739, while its radiation efficiency and total efficiency are approximately 77.6% and 72.0%, respectively. The calculated gain is approximately 3.889 dBi.

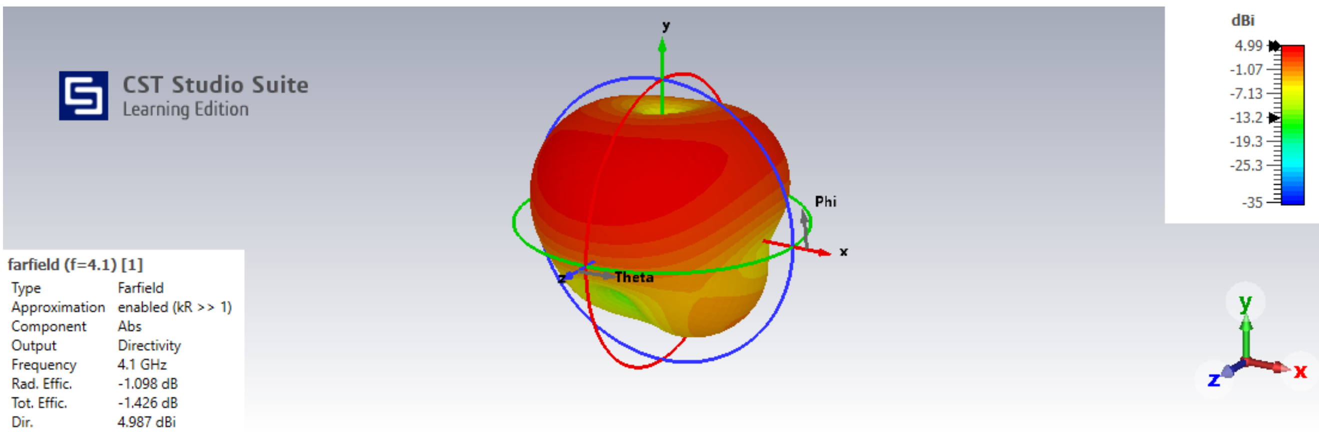

Figure 5: C1 three-dimensional far-field radiation pattern at 4.1 GHz

Received: 22/08/2026; Revised: 28/08/2026; Accepted: 28/08/2026; Published: 31/08/2026

The 4.1 GHz far-field result therefore complements the 3.8 GHz result by demonstrating that the favourable radiation characteristics are maintained in the second operating band. The two selected far-field patterns provide visual evidence that the antenna continues to radiate effectively across both operating regions identified from the S11 analysis.

4.4 Comparison with the Baseline CMSA

The performance of the selected C1 configuration was compared with that of the conventional Circular Microstrip Antenna (CMSA) without metamaterial loading. The conventional CMSA was established as the reference design in the earlier investigation. Over the 3.4–4.2 GHz simulation range, the baseline antenna exhibited directivity between 4.897 and 6.477 dBi and provided a single effective impedance bandwidth of 352.8 MHz, extending from 3.4264 to 3.7792 GHz under the −10 dB criterion.

In contrast, C1 introduces one CSRR into the circular patch and three CSRRs into the ground plane. The resulting configuration produces two distinct −10 dB impedance bands, extending from 3.7056 to 3.8848 GHz and from 3.984 to 4.200 GHz, with bandwidths of 179.2 MHz and 216 MHz, respectively. The combined accepted bandwidth is therefore 395.2 MHz.

Table 6. Comparison of the baseline CMSA and C1

Parameter	**Baseline CMSA**	**C1 with spatially distributed CSRRs**
CSRRs on patch	0	1
CSRRs on ground plane	0	3
Number of operating bands	1	**2**
First operating band	3.4264–3.7792 GHz	3.7056–3.8848 GHz
First-band bandwidth	**352.8 MHz**	179.2 MHz
Second operating band	None	3.984–4.200 GHz
Second-band bandwidth	None	216 MHz
Aggregate accepted bandwidth	**352.8 MHz**	**395.2 MHz**
Maximum reported directivity	6.477 dBi*	5.265 dBi
Operating frequency range investigated	3.4–4.2 GHz	3.4–4.2 GHz

*The baseline value represents the maximum directivity reported over the investigated frequency range, not necessarily its directivity at the same frequency as the C1 maximum.

The comparison reveals an important change in the nature of the antenna response. The conventional CMSA produces one continuous impedance band, whereas the introduction of the four CSRRs transforms the response into two separated operating regions. The C1 configuration therefore does not simply broaden the original resonance. It redistributes the impedance response into two frequency regions.

The aggregate accepted bandwidth increases from 352.8 MHz for the baseline CMSA to 395.2 MHz for C1, corresponding to an increase of approximately 12.0%. At the same time, the C1 response extends to 4.2 GHz, thereby providing a second operating region that is absent from the baseline design. These results indicate that the principal benefit of the selected CSRR arrangement is the modification of the antenna's impedance response and the creation of dual-band operation.

The comparison also shows that the introduction of CSRRs does not automatically produce an increase in directivity. The baseline CMSA has a reported maximum directivity of 6.477 dBi over the investigated range, whereas C1 reaches a maximum of 5.265 dBi at 3.9 GHz. The result is important because it prevents the effect of CSRR integration from being described simply as a general enhancement of all antenna parameters.

Instead, the present results indicate that the spatial distribution of the CSRRs has a stronger and more specific influence on impedance behaviour, producing dual-band operation while maintaining useful radiation characteristics. This observation is consistent with the broader configuration study, in which different numbers and arrangements of CSRRs produced substantially different responses.

4.5 Electromagnetic Interpretation of the CSRR Spatial Arrangement

The comparative results obtained for configurations C1-C4 indicate that the electromagnetic response of the CSRR-loaded circular microstrip antenna depends strongly on the spatial arrangement of the resonators. Although the configurations are derived from the same basic antenna structure, changes in the number and location of the CSRRs produce different impedance responses, operating bands, and matching characteristics. This shows that the effect of CSRR loading cannot be adequately described by the number of resonators alone. Their positions relative to the radiating patch, ground plane, feed structure, and one another are also important design variables.

The electromagnetic behaviour of C1 provides a useful basis for interpreting this effect. C1 contains one CSRR incorporated into the circular patch and three CSRRs incorporated into the ground plane. The resulting

Received: 22/08/2026; Revised: 28/08/2026; Accepted: 28/08/2026; Published: 31/08/2026

S11 response produces two impedance-matched frequency regions, approximately 3.7056-3.8848 GHz and 3.984-4.200 GHz. The occurrence of two distinct operating regions indicates that the CSRR loading modifies the resonant behaviour of the original CMSA and introduces additional electromagnetic interactions within the structure.

A particularly useful observation is obtained at 3.8 GHz, which lies close to the minimum S11 value within the first operating band. At this frequency, the simulated S11 is approximately −11.4 dB, indicating relatively strong impedance matching within the first band. The corresponding surface-current simulation gives a maximum current magnitude of approximately 91.596 A/m. The strong current excitation is consistent with the favourable impedance matching and increased power acceptance indicated by the low S11 value. Since less incident power is reflected at this frequency, a greater proportion of the available input power is coupled into the antenna structure and contributes to the induced electromagnetic currents.

The relationship between the impedance response and the surface-current distribution should, however, be distinguished from directivity. A minimum S11 does not by itself establish maximum directivity. Rather, the low S11 indicates favourable impedance matching and greater power acceptance, while the resulting spatial distribution of the induced currents determines how effectively the accepted power is converted into radiation in different directions. The strong current distribution observed at 3.8 GHz therefore provides electromagnetic evidence of strong excitation of the antenna, while the corresponding far-field and directivity results determine its radiation performance.

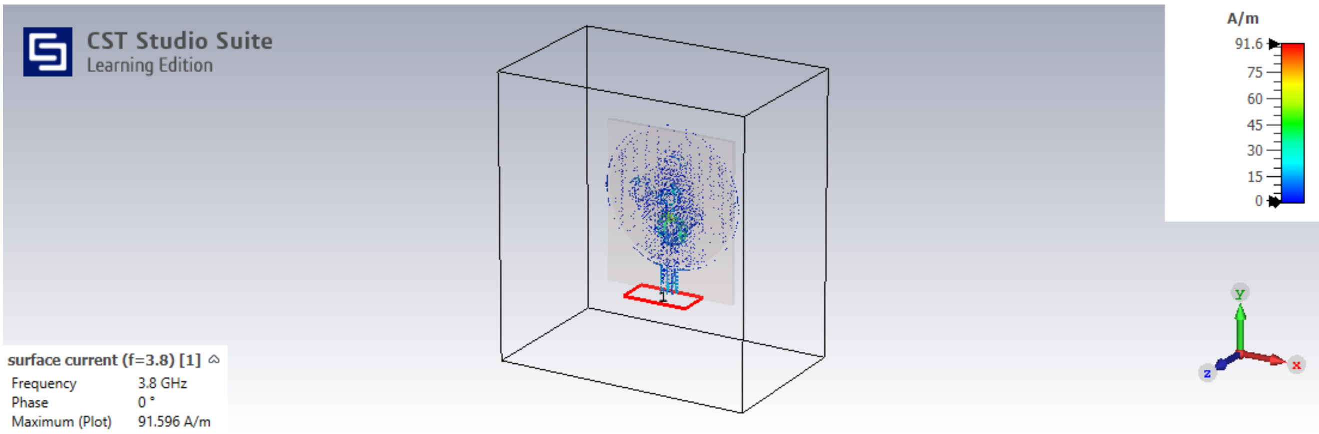

Figure 6. Surface-current distribution of C1 at 3.8 GHz

The second surface-current result, obtained at 4.2 GHz, provides a useful comparison with the first operating region. At this frequency, the antenna remains within the second impedance-matched region, while the maximum simulated surface-current magnitude is approximately 42.521 A/m. The distribution differs from that observed at 3.8 GHz, indicating that the electromagnetic response of the loaded antenna changes with frequency even though the physical arrangement of the CSRRs remains unchanged.

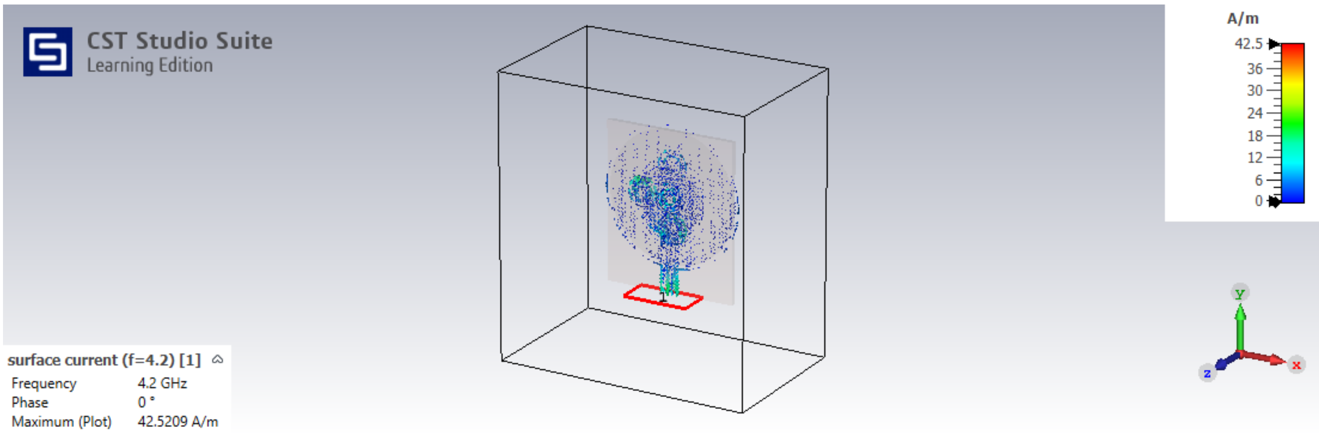

Figure 7. Surface-current distribution of C1 at 4.2 GHz

The difference between the current distributions at 3.8 and 4.2 GHz indicates the frequency-dependent nature of the interaction between the CSRRs and the CMSA. At 3.8 GHz, the strong current excitation occurs near the first resonance of the loaded structure. At 4.2 GHz, the current pattern corresponds to the upper portion of the second operating region and exhibits a different distribution and lower maximum current magnitude. These

Received: 22/08/2026; Revised: 28/08/2026; Accepted: 28/08/2026; Published: 31/08/2026

observations support the view that the two operating bands are associated with different electromagnetic responses of the same CSRR-loaded structure.

The results from C1-C4 further indicate that CSRR quantity and CSRR spatial arrangement should be treated as separate design variables. Configurations having comparable numbers of resonators can produce substantially different S11 and VSWR characteristics because the resonators do not experience identical electromagnetic environments when their positions are changed. Their mutual interaction and their coupling to the patch, ground plane, and feed structure influence the resulting resonant behaviour.

The spatial arrangement therefore provides an additional mechanism for controlling the impedance response of the antenna. Moving a CSRR from one location to another changes the local electromagnetic environment and consequently modifies its coupling with the surrounding structure. The combined response of the coupled patch and CSRR elements determines the location, depth, and separation of the observed resonances. This provides an electromagnetic explanation for the different responses obtained from C1-C4.

For C1, the arrangement of one patch CSRR and three ground-plane CSRRs provides a useful combination of impedance matching and dual-band operation. The surface-current results at 3.8 and 4.2 GHz provide further evidence that the resonators participate in frequency-dependent electromagnetic interactions within the antenna. The observed behaviour supports the conclusion that the simulated performance of the CSRR-loaded CMSA is governed by the spatial distribution and electromagnetic coupling of the resonators, rather than simply by the total number of CSRRs.

This finding is important for subsequent antenna optimisation because it suggests that CSRR placement can be treated as a deliberate design parameter. A systematic study of the geometrical arrangements and their corresponding electromagnetic responses could therefore provide a basis for developing a predictive design approach in which suitable CSRR configurations are selected from their spatial and electromagnetic characteristics rather than exclusively through trial-and-error simulation.

5.0 Conclusion

This study investigated the influence of complementary split-ring resonator (CSRR) spatial arrangement on the electromagnetic performance of a circular microstrip antenna. Four representative configurations, C1-C4, were examined over the 3.4-4.2 GHz frequency range, with variations in the number and placement of CSRRs on the circular patch and ground plane. The simulation results indicate that the electromagnetic response of the CSRR-loaded antenna cannot be explained adequately by the number of resonators alone. Configurations containing comparable numbers of CSRRs exhibited different impedance characteristics, while the configuration with the largest number of CSRRs did not provide the most favourable overall response. These results indicate that the spatial distribution of the resonators is a significant design variable.

The selected C1 configuration, consisting of one CSRR on the circular patch and three CSRRs arranged on the ground plane, exhibited two distinct simulated −10 dB impedance-matched regions from 3.7056-3.8848 GHz and 3.984-4.200 GHz, giving a combined accepted bandwidth of approximately 395.2 MHz. The simulated configuration maintained useful radiation characteristics across the two operating regions, with directivity reaching 5.265 dBi at 3.9 GHz and a calculated maximum gain of approximately 3.965 dBi at 4.2 GHz within the sampled frequencies. The comparison with the conventional CMSA further showed that CSRR loading increased the aggregate accepted bandwidth from 352.8 MHz to 395.2 MHz and transformed the original single-band response into a dual-band response. At the same time, the results show that CSRR integration does not necessarily improve every antenna parameter, since the baseline CMSA exhibited a higher maximum reported directivity.

The surface-current results provide further insight into the observed behaviour. At 3.8 GHz, where C1 exhibits strong impedance matching within the first operating band, the maximum simulated surface-current magnitude was approximately 91.596 A/m. The current distribution at 4.2 GHz was different, indicating that the interaction between the CSRRs and the host antenna varies with frequency. The results therefore suggest that the effect of CSRR loading is strongly associated with the location of the resonators relative to the patch, ground plane, feed structure and existing electromagnetic current distribution. Changing the position of a resonator changes its local coupling environment and consequently modifies the combined resonant response of the antenna.

A significant implication of this study is that CSRR placement should be treated as an independent design parameter rather than as a secondary consequence of CSRR quantity. The findings provide evidence that deliberate manipulation of resonator position can be used to modify impedance behaviour and establish desired operating regions. Further investigation is therefore required to develop a more complete physical understanding of the coupled behaviour of CSRR/SRR structures, surface currents, electromagnetic fields and the host antenna. Such work could establish quantitative relationships between resonator geometry, spatial placement, electromagnetic coupling and the resulting antenna characteristics. This would provide a basis for moving from predominantly trial-and-error CSRR optimisation toward a more predictive design methodology in which resonator arrangements are selected to obtain predefined impedance, bandwidth and radiation characteristics.

Received: 22/08/2026; Revised: 28/08/2026; Accepted: 28/08/2026; Published: 31/08/2026

References

[1] Z. Liu, S. K. Sharma, and Y. M. Gupta, "A survey of microstrip patch antenna design techniques for UWB applications," *Progress in Electromagnetics Research*, vol. 79, pp. 373–414, 2007.

[2] M. Hussain, W. A. Awan, M. S. Alzaidi, N. Hussain, E. M. Ali, and F. Falcone, "Metamaterials and their application in the performance enhancement of reconfigurable antennas: A review," *Micromachines*, vol. 14, no. 2, Art. no. 349, 2023, doi: 10.3390/mi14020349.

[3] E. A. Serria and M. I. Hussein, "Implications of metamaterial on ultra-wide band microstrip antenna performance," *Crystals*, vol. 10, no. 8, Art. no. 677, 2020, doi: 10.3390/cryst10080677.

[4] M. Shobana, "CSRR inspired antenna using artificial neural network for sub 6 GHz 5G applications," *Alexandria Engineering Journal*, vol. 77, pp. 351–367, 2023, doi: 10.1016/j.aej.2023.06.085.

[5] D. Barad, J. C. Dash, D. Sarkar, and P. Srinivasulu, "A CSRR loaded triple-band microstrip patch antenna with suppressed higher order modes for sub-6 GHz phased array application," in *Proc. 2022 IEEE Microwaves, Antennas, and Propagation Conference (MAPCON)*, 2022, doi: 10.1109/MAPCON56011.2022.10046689.

[6] C. J. M. Andrews, "Study on miniaturization of antenna using metamaterials," in *Metamaterials: History, Current State, Applications, and Perspectives*. IntechOpen, 2022, doi: 10.5772/intechopen.106222.

[7] D. Barad, J. C. Dash, D. Sarkar, and P. Srinivasulu, "Dual-band dual-polarized sub-6 GHz phased array antenna with suppressed higher order modes," *Scientific Reports*, vol. 14, Art. no. 6139, 2024, doi: 10.1038/s41598-024-56218-8.

[8] M. Chandrasekhar and K. K. Naik, "Design a dual-band with CSRR cascaded patch antenna array for wireless communications," *Progress In Electromagnetics Research C*, vol. 149, pp. 155–163, 2024, doi: 10.2528/PIERC24090602.

[9] A. Varshney, S. Kumar, D. N. Gençoğlan, S. Tiwari, S. Ara, I. Elfergani, C. Zebiri, and J. Rodriguez, "Compact metasurface antenna for sub-6 GHz applications with isolated n77/n78 bands using CSRR," *Physica Scripta*, vol. 100, no. 1, Art. no. 015508, 2025, doi: 10.1088/1402-4896/ad96f1.

[10] K. Anusha and D. Mohana Geetha, "Miniaturized metamaterial loaded multiband antenna for sub-6 GHz applications," *Indian Journal of Pure & Applied Physics*, vol. 63, no. 6, pp. 488–496, 2025, doi: 10.56042/ijpap.v63i6.15435.

[11] D. R. Basavaraju and S. Ramanujam, "Development of multi-band sub-6 GHz MIMO antenna using complementary split ring resonator and defected ground structure," *International Journal of Engineering Trends and Technology*, vol. 73, no. 11, pp. 312–324, 2025, doi: 10.14445/22315381/IJETT-V73I11P122.

[12] I. A. Oluwafemi, U. Ukommi, E. Ubom, and A. Obot, "Circular microstrip antennas in 5G: Evaluating metamaterial integration," *ABUAD Journal of Engineering Research and Development (AJERD)*, vol. 7, no. 2, pp. 260–269, Sep. 2024, doi: 10.53982/ajerd.2024.0702.25-j.

[13] A. H. Sihvola, *Metamaterials: Physics and Engineering Metamaterials*. Berlin, Germany: Springer, 2007.

[14] J. B. Pendry, A. J. Holden, D. J. Robbins, and W. J. Stewart, "Magnetism from conductors and enhanced nonlinear phenomena," *IEEE Transactions on Microwave Theory and Techniques*, vol. 47, no. 11, pp. 2075–2084, 1999, doi: 10.1109/22.798002.

Received: 22/08/2026; Revised: 28/08/2026; Accepted: 28/08/2026; Published: 31/08/2026